AGU PUBLICATIONS

Geophysical Research Letters

RESEARCH LETTER
10.1002/2014GL060533

Key Points:
- InSAR-measured surface subsidence can be used to assess tundra fire impacts
- Both active layer thickening and permafrost thawing increased surface subsidence
- InSAR offers a new tool to understand postfire permafrost dynamics

Supporting Information:
- Readme
- Table S1
- Figure S1
- Figure S2

Correspondence to:
L. Liu,
liulin@cuhk.edu.hk

Citation:
Liu, L., E. E. Jafarov, K. M. Schaefer, B. M. Jones, H. A. Zebker, C. A. Williams, J. Rogan, and T. Zhang (2014), InSAR detects increase in surface subsidence caused by an Arctic tundra fire, *Geophys. Res. Lett.*, *41*, 3906–3913, doi:10.1002/2014GL060533.

Received 14 MAY 2014
Accepted 16 MAY 2014
Accepted article online 20 MAY 2014
Published online 2 JUN 2014

InSAR detects increase in surface subsidence caused by an Arctic tundra fire

Lin Liu[1], Elchin E. Jafarov[2], Kevin M. Schaefer[2], Benjamin M. Jones[3], Howard A. Zebker[4], Christopher A. Williams[5], John Rogan[5], and Tingjun Zhang[2,6]

[1]Earth System Science Programme, Faculty of Science, Chinese University of Hong Kong, Hong Kong, China, [2]National Snow and Ice Data Center, Cooperative Institute for Research in Environmental Sciences, University of Colorado Boulder, Boulder, Colorado, USA, [3]Alaska Science Center, U.S. Geological Survey, Anchorage, Alaska, USA, [4]Department of Geophysics, Stanford University, Stanford, California, USA, [5]Graduate School of Geography, Clark University, Worcester, Massachusetts, USA, [6]College of Earth and Environmental Sciences, Lanzhou University, Lanzhou, China

Abstract Wildfire is a major disturbance in the Arctic tundra and boreal forests, having a significant impact on soil hydrology, carbon cycling, and permafrost dynamics. This study explores the use of the microwave Interferometric Synthetic Aperture Radar (InSAR) technique to map and quantify ground surface subsidence caused by the Anaktuvuk River fire on the North Slope of Alaska. We detected an increase of up to 8 cm of thaw-season ground subsidence after the fire, which is due to a combination of thickened active layer and permafrost thaw subsidence. Our results illustrate the effectiveness and potential of using InSAR to quantify fire impacts on the Arctic tundra, especially in regions underlain by ice-rich permafrost. Our study also suggests that surface subsidence is a more comprehensive indicator of fire impacts on ice-rich permafrost terrain than changes in active layer thickness alone.

1. Introduction

Fire is a major disturbance in Arctic tundra and boreal forests with a significant impact on soil hydrology, carbon cycling, and permafrost [*Balshi et al.*, 2009]. Tundra fires can trigger and promote permafrost degradation, manifested by thickening of the active layer [*Rocha and Shaver*, 2011], defined as the top soil layer undergoing seasonal freeze-thaw cycles. Active layer thickness (ALT) increases after a fire due to decreased albedo and a thinner surface organic layer. Exposed soil and ash darken the surface and increase absorption of shortwave radiation, resulting in higher soil temperatures and therefore a larger ALT [*Hinzman et al.*, 1991]. Moreover, a thick surface layer of organic soil can insulate and protect permafrost from thaw; but fires typically burn off a portion of this organic layer, further thickening the active layer [*Yoshikawa et al.*, 2002; *Mack et al.*, 2011; *Jafarov et al.*, 2013].

Tundra fires may also promote ice-wedge degradation [*Jones et al.*, 2013] and trigger thermokarst and thaw-related landscape features [*Mann et al.*, 2010]. Thermokarst, defined as "the process by which characteristic landforms result from the thawing of ice-rich permafrost or the melting of massive ice" [*Harris et al.*, 1988; *van Everdingen*, 1998], is important to vegetation succession, hydrology, and carbon cycling in permafrost regions. Thermokarst processes can expand lakes, drain lakes, accelerate thaw, disturb the soil column, and promote erosion, all of which will increase CO_2 and CH_4 emissions [*Koven et al.*, 2011; *Grosse et al.*, 2013]. Thermokarst lakes and wetlands are the dominant natural source of CH_4 in permafrost regions [*Walter et al.*, 2007].

Tundra fires cause surface subsidence by two major mechanisms: increase in ALT and thawing of ice-rich permafrost. The freezing of soil water and melting of ground ice within the active layer produces subsidence in summer and frost heave in winter, resulting in a typical seasonal surface vertical deformation on the North Slope of Alaska of 1–4 cm [*Little et al.*, 2003; *Liu et al.*, 2010]. A thicker active layer typically contains more water, therefore producing larger subsidence during the thaw season. Additionally, in areas underlain by ice-rich permafrost, fire-induced thermal disturbance may melt ground ice, resulting in either gentle, continuous subsidence as the entire active layer soil settles due to top-down thawing of the permafrost layer [*Nelson et al.*, 2001; *Liu et al.*, 2010], or local, irregular subsidence, which can lead to the formation of various thermokarst terrains [*Jorgenson*, 2013]. Collectively, we use "permafrost thaw subsidence" in this paper to refer to the surface subsidence due to thawing of ice-rich permafrost, without further distinguishing whether it is gentle and spatially regular or localized and irregular.

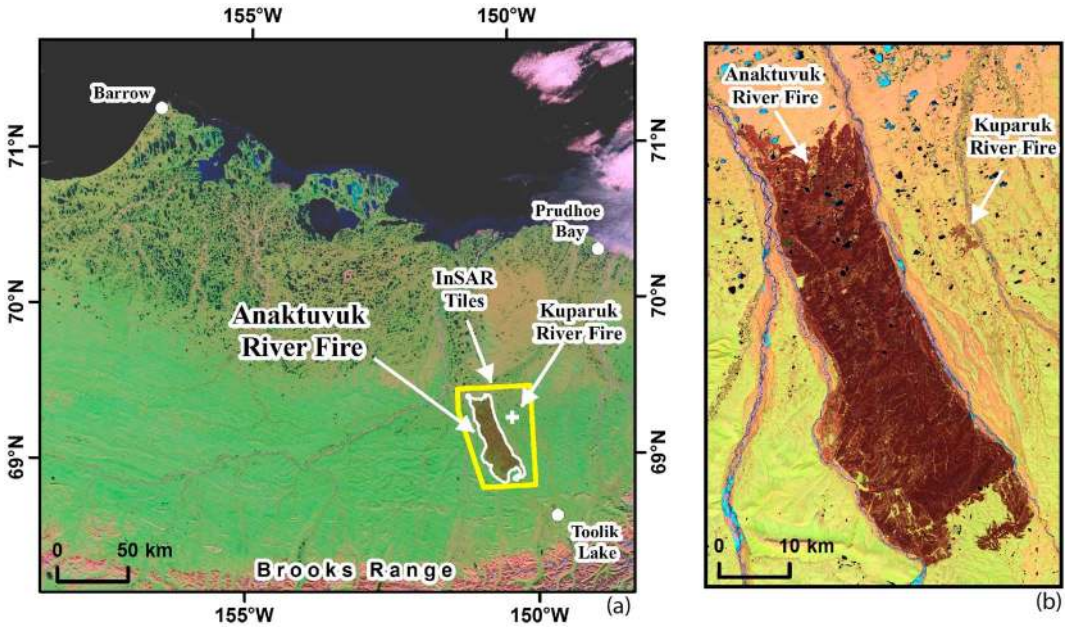

Figure 1. (a) MODIS image acquired in 2008 showing the location of the Anaktuvuk River (white polygon) and Kuparuk River (white cross) fires on the North Slope of Alaska. The yellow box outlines boundary of InSAR maps in Figures 2 and 3. (b) A Landsat-5 TM image acquired in 2008 demonstrating the change in surface albedo that resulted from the tundra fire.

Satellite or aerial optical imagery is widely used to map fire burn extent, severity, and recovery. Optical remote sensing is especially useful for fires in remote areas such as the Arctic. Several spectral indices, such as the differential Normalized Burn Ratio, have been developed to measure fire severity [e.g., *Rogan and Yool*, 2001; *Key and Benson*, 2006; *Boelman et al.*, 2011; *Kolden and Rogan*, 2013; *Loboda et al.*, 2013]. However, optical remote sensing cannot measure ground subsidence caused by tundra fires. It is therefore desirable for alternative and quantitative remote sensing methods and products to complement optical products.

The objective of this study is to quantify and understand fire-induced surface subsidence in Arctic tundra using Interferometric Synthetic Aperture Radar (InSAR). Because it operates at microwave frequency, InSAR is capable of imaging ground targets in all weather conditions. InSAR has been used to map fire burn areas and assess fire impacts such as vegetation loss in boreal forests [e.g., *Liew et al.*, 1999; *Balzter*, 2001], but to the best of our knowledge, not in tundra systems. Here we demonstrate, for the first time, the effectiveness of InSAR to quantify fire-induced ground subsidence during thaw seasons after the 2007 Anaktuvuk River tundra fire event on the North Slope of Alaska, USA.

2. Methods

In this section, we describe our study site (section 2.1), followed by a brief summary of the InSAR time series analysis that addresses the limitation of the InSAR technique due to loss of interferometric coherence caused by the fire (section 2.2). The changes in surface subsidence could be caused by changes in ALT and permafrost thaw subsidence (hereafter referred as the "ALT contribution" and the "permafrost contribution," respectively); however, this study's InSAR measurements alone cannot separate these two factors. Our method was to use ground-based ALT measurements and a model proposed by *Liu et al.* [2012] to predict the ALT contribution and then to estimate the permafrost contribution using the difference between the InSAR-observed subsidence change and the ALT contribution (section 2.3).

2.1. Study Site: Anaktuvuk River Fire

The Anaktuvuk River fire occurred about 60–100 km northwest of the Toolik Lake Research Station on the North Slope of Alaska (Figure 1). Ignited by lightning on 16 July 2007, the fire initially burned slowly at ~0.62 km^2/d, accelerated to ~70 km^2/d in early September, and finally ceased in early October [*Jones et al.*,

2009]. It burned ~1039 km^2 of tundra area, doubling the cumulative area burned on the North Slope in the past 50 years [*Jones et al.*, 2009]. The fire released ~2.1 Tg of carbon into the atmosphere, which is roughly equal to the annual net carbon sink for the entire circumpolar Arctic tundra [*Mack et al.*, 2011]. A much smaller fire, the Kuparuk River fire, was about 10 km to the east of the Anaktuvuk River fire (Figure 1). The Kuparuk River fire also started in July 2007, but burned for about a week, combusting ~7.2 km^2 at low severity [*Jones et al.*, 2009].

Field measurements show a partial loss of the surface organic soil horizon due to the Anaktuvuk River fire. According to the postfire surveys conducted by *Mack et al.* [2011], the reduction of organic soils was limited to the surface of the organic layer. The reduction of organic layer thickness is related to the burn severity, which, therefore, varies spatially. Averaged over sites with different burn severity, the organic layer thickness decreased by ~6 cm, with ~15 cm remaining after the fire [*Mack et al.*, 2011].

Field measurements also indicate an increase of ALT due to the fire. Since ALT is rarely measured before a fire, difference in ALT between burned and unburned sites is typically used to quantify the fire impacts on permafrost. ALT was generally larger at burned sites than at unburned sites by 10 to 20 cm, largely due to thawing of the mineral soil layer below the organic layer [*Rocha and Shaver*, 2011; *Jandt et al.*, 2012; *Bret-Harte et al.*, 2013].

2.2. InSAR Time Series Analysis

Using the radar phase from two or more synthetic aperture radar (SAR) images, InSAR maps surface deformation at high spatial resolution (typically 10 m or higher). Time series analyses of regional InSAR deformation maps have been used to retrieve seasonal and long-term surface subsidence in permafrost regions [*Liu et al.*, 2010, 2014; *Short et al.*, 2011; *Chen et al.*, 2013]. In this study we used Phased Array type L-band Synthetic Aperture Radar (PALSAR) images acquired by the Japanese Advanced Land Observing Satellite (ALOS) from 2006 to 2010 (listed in Table S1 in the supporting information). All images are in the fine beam and horizontal-horizontal (HH) polarization mode. For each image acquisition, we concatenated two adjacent SAR frames (1380 and 1390) in Track 255 to provide a complete, seamless coverage of the study area. We then conducted InSAR processing using a software package developed at Stanford University [*Zebker et al.*, 2010] and produced 34 deformation maps, namely interferograms (see Figure S1).

InSAR's capability and accuracy for subsidence measurements are limited by the problem of coherence loss. Interferometric coherence, which ranges from zero to one, is a statistical comparison between two radar echoes from different SAR images [*Li and Goldstein*, 1990]. Radar echoes from different SAR images are correlated with each other (i.e., high coherence) if they represent the same interaction with the same set of ground scatters inside an image pixel size. It is well known that fire burn results in coherence loss, simply because of the dramatic change of surface scattering from tundra vegetation to burned surface materials [e.g., *Liew et al.*, 1999]. Our coherence analysis over the Anaktuvuk River fire confirms the fire-induced coherence loss, which are well bounded by the fire perimeter (see Figure S2 in the supporting information). Therefore, we were unable to directly quantify surface subsidence during the fire.

Alternatively, we measured changes of thaw-season ground subsidence before and after the fire. Relatively good coherence is maintained in the interferograms that spanned prefire or postfire seasons, making it possible to conduct InSAR time series analysis from 2006 to 2010. Accordingly, we revised the InSAR time series analysis method developed previously [*Liu et al.*, 2012] to quantify changes in seasonal subsidence associated with the Anaktuvuk River fire. Specifically, we modeled the InSAR-measured ground subsidence (D) between two dates t_1 and t_2 as

$$D = \left(E_2\sqrt{A_2} - E_1\sqrt{A_1}\right) + B_\perp K, \tag{1}$$

where $E_{1,2}$ is the seasonal coefficient with the subscripts corresponding to the two dates (more below and in equation (2)), $A_{1,2}$ is the accumulated degree day of thawing (ADDT), calculated using air temperature recorded at Toolik Lake Research Station [*Environmental Data Center*, 2014]; $B_\perp$ is the perpendicular baseline; and K is a variable determined by the errors in the digital elevation model used in the InSAR processing.

Here we only point out the major differences from the *Liu et al.* [2012] study. First, we did not include a linear trend in surface subsidence because the PALSAR images only spanned 4 years, which is an insufficient time

period in which to measure statistically significant trends. Second, we assumed that seasonal coefficients are different during prefire and postfire years, but are constant in each period. We used the following expression for $E_{i,(i\,=\,1,2)}$:

$$E_i = \begin{cases} E_{\text{pre}} & t_i < T_0 \\ E_{\text{post}} & t_i \geq T_0 \end{cases}, \tag{2}$$

where E_{pre} and E_{post} are the two constants corresponding to prefire and postfire years, separated by T_0, which is set as 1 September 2007.

Using all 34 interferograms with various spans, we were able to solve for three unknowns, K, E_{pre}, and E_{post}, and their uncertainties. We then calculated the averaged seasonal subsidence during prefire and postfire thaw seasons (denoted as δ_{pre} and δ_{post}, respectively), by using E_{pre}, E_{post}, their corresponding ADDTs, and a geometric factor for mapping line-of-sight direction to vertical direction (see *Liu et al.* [2012] for more details). The 34 interferograms we used include the span-fire ones for mapping subsidence outside the fire zones.

2.3. Predicting Seasonal Subsidence Using Ground-Measured ALT

To interpret and understand the InSAR-observed subsidence changes, we predicted the ALT contribution to total subsidence from ground-measured ALT. Ideally, one should use the temporal changes of ALT before and after the fire in the modeling effort. However, since no ALT measurements were made in the study area before the fire, we instead used ALT measured at 25 sites using mechanical probing after the fire during 2008–2010 [*Rocha and Shaver*, 2011; *Jandt et al.*, 2012] and only modeled the postfire seasonal subsidence. To compare with the two-dimensional InSAR maps, we extrapolated all site measurements to a continuous ALT grid inside the Anaktuvuk River fire zone, using a curvature surface gridding algorithm provided by the Generic Mapping Tools [*Wessel and Smith*, 1998]. Because there is only one ALT site located inside the Kuparuk River fire, we assigned a constant ALT of 38 cm locally just for this fire.

We then predicted the postfire thaw-season subsidence using a model developed by *Liu et al.* [2012]. Their model attributes the seasonal subsidence (δ) as purely caused by volume change of water in the active layer from ice to liquid water. Such a relationship can be described by this integral:

$$\delta = \int_0^{\text{ALT}} PS \frac{\rho_w - \rho_i}{\rho_i}\, \mathrm{d}h, \tag{3}$$

where P is the soil porosity, S is the soil moisture fraction of saturation, ρ_w is the density of water, ρ_i is the density of ice, and dh is the incremental thickness of the thawed soil column. For simplicity, we assumed that the active layer is saturated ($S = 1.0$) and therefore ALT from equation (3) relationship is determined by the vertical distribution of porosity in the active layer soil column. This calculation overestimates δ in places where active layer is unsaturated; in other words, it gives the upper bound on δ.

We assumed a two-layered soil model for the postfire active layer. According to soil surveys, even though some organic soil were combusted during the fire, the active layer still has an organic layer remaining on top and a mineral layer lying below [*Mack et al.*, 2011; *Bret-Harte et al.*, 2013]. Although the absolute thickness of the organic and mineral layers varies spatially due to the heterogeneity of soil composition and burn severity, the percentile between the two layers is relatively a constant 25% versus 75% [*Bret-Harte et al.*, 2013]. We therefore used this model by fixing the percentile and varying the total thickness set by the extrapolated ALT. In summary, this model takes the loss of the top organic layer into account and represents the average soil properties at the moderately and severely burned areas.

Our prediction provides a first-order, averaged approximation to the complex fire-burned landform and active layer soils. The predicted subsidence is relatively insensitive to the assumed soil compositions as long as an organic layer is included. We also estimated the uncertainties in the predicted subsidence due to a combination of InSAR measurement uncertainties and model parameter uncertainties. More details can be found in *Liu et al.* [2012].

3. Results

We observed a large increase in surface subsidence inside the fire zone. In prefire years, the magnitude of thaw-seasonal subsidence ranges from 1 to 4 cm (Figure 2a), consistent with the previous assessments near

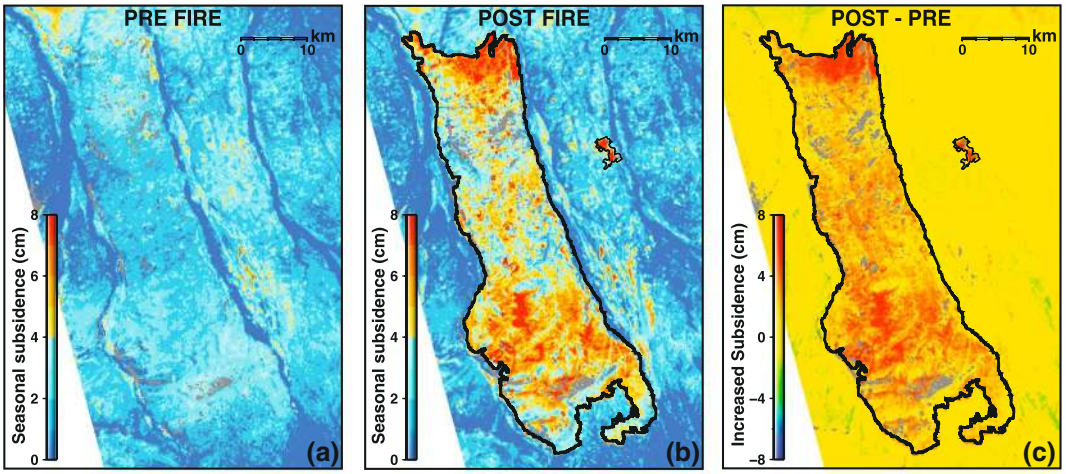

Figure 2. Thaw-season subsidence averaged during (a) prefire years and (b) postfire years, respectively. Grey areas represent unreliable subsidence measurements caused by coherence loss. (c) The difference between postfire and prefire subsidence, i.e., Figure 2b minus Figure 2a. Perimeters of both Anaktuvuk River and Kuparuk River fires are outlined in Figures 2b and 2c, based on a Landsat-5 image.

Prudhoe Bay [*Little et al.*, 2003; *Liu et al.*, 2010]. By contrast, thaw-seasonal subsidence in postfire years (Figure 2b) shows a distinct increase inside both the Anaktuvuk and Kuparuk River fires compared to the surrounding unburned tundra areas. The postfire subsidence minus the prefire subsidence indicates an increased subsidence that ranges from 2 to 8 cm (Figure 2c). We found no significant changes in subsidence outside these two fire zones (Students' t test, $P < 0.01$). Because we included interferograms that spanned the fire over the surrounding unburned area than the burned areas, subsidence at the unburned areas is generally more accurate (Figure 3).

The gridded postfire ALT map shows a variation between 30 cm and 70 cm inside the Anaktuvuk River fire zone (Figure 4a). Since this map is an extrapolation based on ALT measured at sparse ground sites, it is smoothed and may not fully represent potentially large spatial variability. Additionally, the sites are unevenly distributed, which partly determines the spatial pattern of the extrapolated field.

The predicted postfire thaw subsidence shows a gentle variation from 2 ± 1 cm to 4 ± 1 cm (Figure 4b). As explained in section 2.3, this only includes the effect caused by melting of pore ice in active layer with thickness defined by Figure 4a. This prediction is much smaller than the InSAR-observed postfire subsidence as shown in Figure 2b.

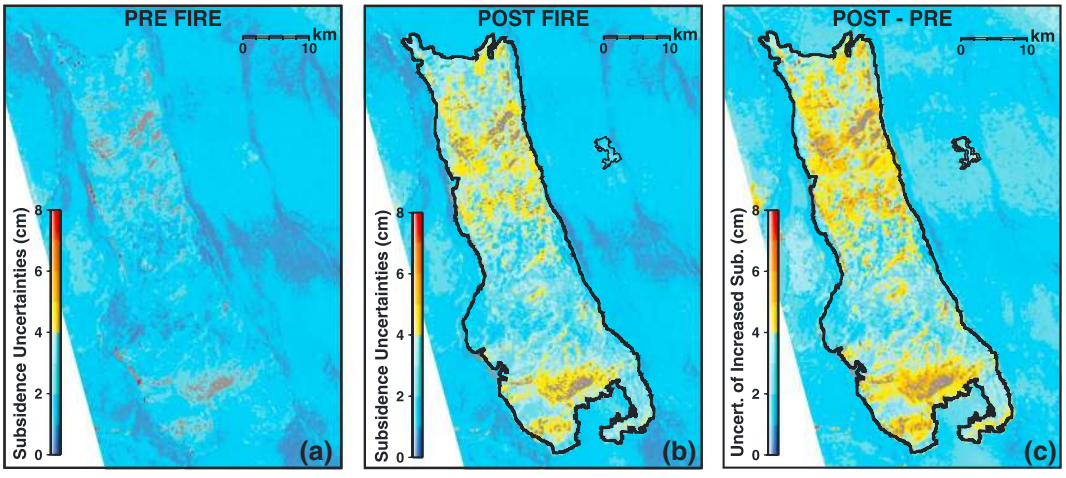

Figure 3. Estimated uncertainties (1σ) of the seasonal subsidence in prefire, postfire years, and their changes, corresponding to the ones shown in Figure 2.

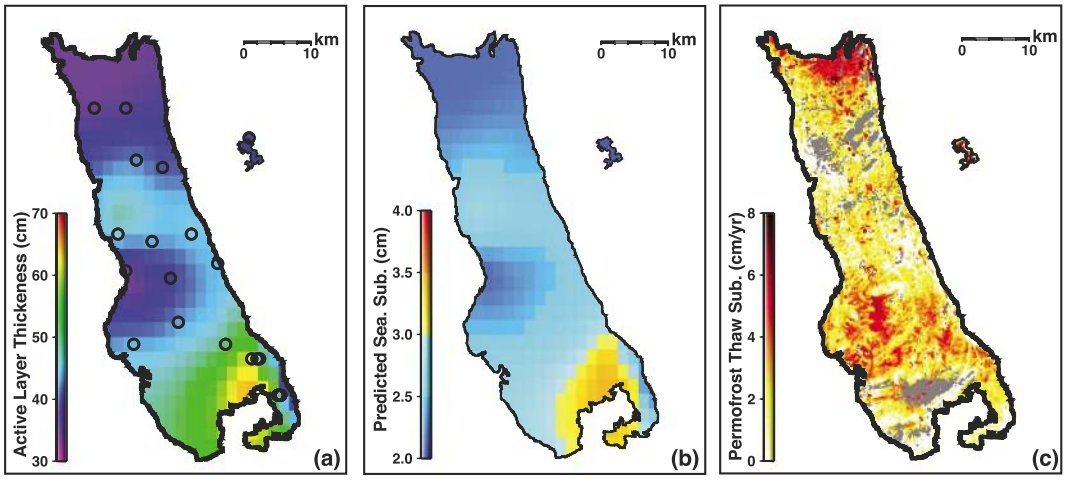

Figure 4. (a) Averaged 2008–2010 active layer thickness inside the fire zones, extrapolated from in situ measurements at sites marked by circles. (b) Predicted thaw-seasonal ground subsidence in postfire years (see text), for comparison with Figure 2b. (c) Estimated ground subsidence due to thawing of ice-rich permafrost.

4. Discussion

We attributed the discrepancy between the observed postfire subsidence and the predicted ALT contribution as the contribution from thawing ice-rich permafrost, shown in Figure 4c. Ice-rich permafrost is abundant in this area [*Jorgenson and Grunblatt*, 2013]. Field investigations have found ice-wedge degradation and thermokarst features such as gullies and small landslides formed after the fire [*Mann et al.*, 2010; *Jones et al.*, 2013]. The spatial variability of our estimated permafrost thaw subsidence is determined by the spatial and vertical distribution of ice-rich permafrost, ice content, microtopography, and surface hydrology. These local factors, however, are poorly constrained, making it challenging to further investigate the causes and consequences of the spatial variability in a quantitative manner.

Our method assumes a linear permafrost thaw subsidence rate during 2008–2010, although the actual response is more likely to be nonlinear, with the largest subsidence occurring immediately following the fire. If we had a long time series (e.g., longer than 10 years) of interferograms with high sampling rates (e.g., higher than one measurement per month), it would be possible to statistically separate changes in ALT from permafrost thaw subsidence from the InSAR data only, as demonstrated in *Liu et al.* [2010].

Another limitation of using InSAR to map permafrost thaw subsidence is the issue of coherence loss. Top-down thawing of permafrost may result in coherent surface subsidence that is widespread [*Shiklomanov et al.*, 2013]. However, other types of permafrost thaw subsidence, widely known as thermokarst depressions, could be localized and irregular and its magnitude could be tens of centimeters or even a few meters within a thaw season [*Short et al.*, 2011]. Additionally, thermokarst subsidence is often accompanied by surface soil erosion. All these factors would result in loss of coherence, prohibiting reliable subsidence measurements. In reality, the permafrost thaw subsidence could be large at the low-coherence areas shown in Figure 4c and requires further investigation.

Fire-induced surface subsidence could also be caused by loss of the organic layer. For instance, *Mack et al.* [2011] estimated a loss of organic layer thickness of about 6 cm by comparing organic layer thickness measured at unburned and burned sites inside the Anaktuvuk River fire burn zone. However, we were unable to detect such changes due to the coherence loss in span-fire interferograms. In other words, our InSAR-measured subsidence may actually underestimate the total ground subsidence due to the fire.

5. Conclusions

Using L band PALSAR data on the Anaktuvuk River fire, we demonstrated that InSAR is an effective and unique technique for assessing impacts of Arctic tundra fires that occur in ice-rich permafrost terrain. We found an increase of up to 8 cm of thaw-season ground subsidence in response to the fire disturbance, despite the issues associated with coherence loss during the fire. This is likely caused by a combination of

both active layer thickening and permafrost thaw subsidence as a result of melting ground ice in permafrost, with the latter contributing the most. Our study suggests that surface subsidence is a more comprehensive indicator of fire impacts on ice-rich permafrost terrain than active layer thickening alone.

Acknowledgments

We thank A. Rocha and two anonymous reviewers for their insightful comments. The ALOS PALSAR data are copyrighted by the Japan Aerospace Exploration Agency and provided by the Alaska Satellite Facility, University of Alaska Fairbanks. Data for all figures in this paper are freely available upon request to L. Liu. This study was supported by the U.S. NSF grants ARC-1204013, ARC 1204167, and ARC-0901962 and the U.S. NASA grant NNX13AM25G. Any use of trade, product, or firm names is for descriptive purposes only and does not imply endorsement by the U.S. Government.

The Editor thanks two anonymous reviewers for their assistance in evaluating this paper.

References

Balshi, M. S., A. D. McGuire, P. Duffy, M. Flannigan, J. Walsh, and J. Melillo (2009), Assessing the response of area burned to changing climate in western boreal North America using a multivariate adaptive regression splines (MARS) approach, *Global Change Biol.*, *15*(3), 578–600, doi:10.1111/j.1365-2486.2008.01679.x.

Balzter, H. (2001), Forest mapping and monitoring with interferometric synthetic aperture radar (InSAR), *Prog. Phys. Geogr.*, *25*(2), 159–177, doi:10.1177/030913330102500201.

Bret-Harte, M. S., M. C. Mack, G. R. Shaver, D. C. Huebner, M. Johnston, C. A. Mojica, C. Pizano, and J. A. Reiskind (2013), The response of Arctic vegetation and soils following an unusually severe tundra fire, *Philos. Trans. R. Soc. London, Ser. B*, *368*(1624), 20120490, doi:10.1098/rstb.2012.0490.

Boelman, N. T., A. V. Rocha, and G. R. Shaver (2011), Understanding burn severity sensing in Arctic tundra: Exploring vegetation indices, suboptimal assessment timing and the impact of increasing pixel size, *Int. J. Remote Sens.*, *32*(22), 7033–7056, doi:10.1080/01431161.2011.611187.

Chen, F. L., H. Lin, W. Zhou, T. H. Hong, and G. Wang (2013), Surface deformation detected by ALOS PALSAR small baseline SAR interferometry over permafrost environment of Beiluhe section, Tibet Plateau, China, *Remote Sens. Environ.*, *138*, 10–18, doi:10.1016/j.rse.2013.07.006.

Environmental Data Center Team (2014), Meteorological monitoring program at Toolik, Alaska, Toolik Field Station, Institute of Arctic Biology, Univ. of Alaska Fairbanks, Fairbanks, AK 99775. [Available at http://toolik.alaska.edu/edc/abiotic_monitoring/data_query.php.]

Grosse, G., B. M. Jones, and C. D. Arp (2013), Thermokarst lake, drainage, and drained basins, in *Treatise on Geomorphology*, edited by J. Shroder, R. Giardino, and J. Harbor, pp. 1–29, Elsevier Academic Press, San Diego, Calif.

Harris, S. A., H. M. French, J. A. Heginbottom, G. H. Johnston, B. Ladanyi, D. C. Sego, and R. O. van Everdingen (1988), *Glossary of Permafrost and Related Ground-Ice Terms*, *Tech. Memo.*, vol. 142, National Research Council of Canada, Ottawa, Canada.

Hinzman, L., D. Kane, R. Gieck, and K. Everett (1991), Hydrologic and thermal properties of the active layer in the Alaskan Arctic, *Cold Reg. Sci. Technol.*, *19*(2), 95–110, doi:10.1016/0165-232X(91)90001-W.

Jafarov, E. E., V. E. Romanovsky, H. Genet, A. D. McGuire, and S. S. Marchenko (2013), The effects of fire on the thermal stability of permafrost in lowland and upland black spruce forests of interior Alaska in a changing climate, *Environ. Res. Lett.*, *8*(3), 035030, doi:10.1088/1748-9326/8/3/035030.

Jandt, R. R., E. A. Miller, D. A. Yokel, M. S. Bret-Harte, M. C. Mack, and C. A. Kolden (2012), Findings of Anaktuvuk River fire recovery study 2007–2011, US Bureau of Land Management, 39 pp.

Jones, B. M., C. A. Kolden, R. Jandt, J. T. Abatzoglou, F. Urban, and C. D. Arp (2009), Fire behavior, weather, and burn severity of the 2007 Anaktuvuk River tundra fire, North Slope, Alaska, *Arct. Antarct. Alp. Res.*, *41*(3), 309–316, doi:10.1657/1938-4246-41.3.309.

Jones, B. M., A. L. Breen, B. V. Gaglioti, D. H. Mann, A. V. Rocha, G. Grosse, C. D. Arp, M. L. Kunz, and D. A. Walker (2013), Identification of unrecognized tundra fire events on the north slope of Alaska, *J. Geophys. Res. Biogeosci.*, *118*, 1334–1344, doi:10.1002/jgrg.20113.

Jorgenson, M. T. (2013), Thermokarst terrains, in *Treatise on Geomorphology*, Glacial and Periglacial Geomorphology, vol. 8, edited by J. Shroder, R. Giardino, and J. Harbor, pp. 313–324, Academic Press, San Diego, Calif.

Jorgenson, M. T., and J. Grunblatt (2013), Landscape-level ecological mapping of northern Alaska and field site photography, Report prepared for the Arctic Landscape Conservation Cooperative. [Available at http://arcticlcc.org/assets/products/ALCC2011-06/reports/NorthernAK_Landscape_Mappping_Field_Photos_Final_RPT.pdf.]

Key, C. H., and N. C. Benson (2006), Landscape assessment: Ground measure of severity, the composite burn index, and remote sensing of severity, the normalized burn ratio, in *FIREMON: Fire Effects Monitoring and Inventory System*, edited by D. C. Lutes et al., USDA Forest Service, Rocky Mountain Research Station, Ogden, Utah, *General Technical Repor*t RMRS-GTR-164-CD: LA1–LA51.

Kolden, C., and J. Rogan (2013), Mapping wildfire burn severity in the Arctic tundra from downsampled MODIS data, *Arct. Antarct. Alp. Res.*, *45*, 64–76.

Koven, C. D., B. Ringeval, P. Friedlingstein, P. Ciais, P. Cadule, D. Khvorostyanov, G. Krinner, and C. Tarnocai (2011), Permafrost carbon-climate feedbacks accelerate global warming, *Proc. Natl. Acad. Sci. U.S.A.*, *108*(36), 14,769–14,774, doi:10.1073/pnas.1103910108.

Li, F. K., and R. Goldstein (1990), Studies of multibaseline spaceborne interferometric synthetic aperture radars, *IEEE Trans. Geosci. Remote Sens.*, *28*(1), 88–97, doi:10.1109/36.45749.

Liew, S. C., L. K. Kwoh, K. Padmanabhan, O. K. Lim, and H. Lim (1999), Delineating land/forest fire burnt scars with ERS interferometric synthetic aperture radar, *Geophys. Res. Lett.*, *26*(16), 2409–2412, doi:10.1029/1999GL900189.

Little, J., H. Sandall, M. Walegur, and F. Nelson (2003), Application of Differential Global Positioning Systems to monitor frost heave and thaw settlement in tundra environments, *Permafrost Periglacial Processes*, *14*(4), 349–357, doi:10.1002/ppp.466.

Liu, L., T. Zhang, and J. Wahr (2010), InSAR measurements of surface deformation over permafrost on the North Slope of Alaska, *J. Geophys. Res.*, *115*, F03023, doi:10.1029/2009JF001547.

Liu, L., K. Schaefer, T. Zhang, and J. Wahr (2012), Estimating 1992–2000 average active layer thickness on the Alaskan North Slope from remotely sensed surface subsidence, *J. Geophys. Res.*, *117*, F01005, doi:10.1029/2011JF002041.

Liu, L., K. Schaefer, A. Gusmeroli, G. Grosse, B. M. Jones, T. Zhang, A. D. Parsekian, and H. A. Zebker (2014), Seasonal thaw settlement at drained thermokarst lake basins, Arctic Alaska, *Cryosphere*, *7*, 815–826, doi:10.5194/tc-8-815-2014.

Loboda, T., N. French, C. Hight-Harf, L. Jenkins, and M. Miller (2013), Mapping fire extent and burn severity in Alaskan tussock tundra: An analysis of the spectral response of tundra vegetation to wildland fire, *Remote Sens. Environ.*, *134*, 194–209, doi:10.1016/j.rse.2013.03.003.

Mack, M. C., M. S. Bret-Harte, T. N. Hollingsworth, R. R. Jandt, E. A. Schuur, G. R. Shaver, and D. L. Verbyla (2011), Carbon loss from an unprecedented Arctic tundra wildfire, *Nature*, *475*(7357), 489–492.

Mann, D. H., P. Groves, R. E. Reanier, and M. L. Kunz (2010), Floodplains, permafrost, cottonwood trees, and peat: What happened the last time climate warmed suddenly in arctic Alaska?, *Quat. Sci. Rev.*, *29*(27), 3812–3830, doi:10.1016/j.quascirev.2010.09.002.

Nelson, F. E., O. A. Anisimov, and N. I. Shiklomanov (2001), Subsidence risk from thawing permafrost, *Nature*, *410*(6831), 889–890.

Rocha, A. V., and G. R. Shaver (2011), Postfire energy exchange in arctic tundra: The importance and climatic implications of burn severity, *Global Change Biol.*, *17*(9), 2831–2841, doi:10.1111/j.1365-2486.2011.02441.x.

Rogan, J., and S. R. Yool (2001), Mapping fire-induced vegetation depletion in the Peloncillo Mountains, Arizona and New Mexico, *Int. J. Remote Sens.*, *22*(16), 3101–3121, doi:10.1080/01431160152558279.

Shiklomanov, N. I., D. A. Streletskiy, J. D. Little, and F. E. Nelson (2013), Isotropic thaw subsidence in undisturbed permafrost landscapes, *Geophys. Res. Lett.*, *40*, 6356–6361, doi:10.1002/2013GL058295.

Short, N. B., N. Brisco, W. Couture, K. M. Pollard, and P. Budkewitsch (2011), A comparison of TerraSAR-X, RADARSAT-2 and ALOS-PALSAR interferometry for monitoring permafrost environments, case study from Herschel Island, Canada, *Remote Sens. Environ.*, *115*(12), 3491–3506.

van Everdingen, R. (1998), *Multi-Language Glossary of Permafrost and Related Ground-Ice Terms*, National Snow and Ice Data Center/World Data Center for Glaciology, Boulder, Colo. [Available at http://nsidc.org/fgdc/glossary/english.html.]

Walter, K. M., L. C. Smith, and F. S. Chapin (2007), Methane bubbling from northern lakes: Present and future contributions to the global methane budget, *Philos. Trans. R. Soc. Ser. A*, *365*, 1657–1676, doi:10.1098/rsta.2007.2036.

Wessel, P., and W. H. F. Smith (1998), New, improved version of generic mapping tools released, *Eos Trans. AGU*, *79*(47), 579–579, doi:10.1029/98EO00426.

Yoshikawa, K., W. R. Bolton, V. E. Romanovsky, M. Fukuda, and L. D. Hinzman (2002), Impacts of wildfire on the permafrost in the boreal forests of Interior Alaska, *J. Geophys. Res.*, *107*(D1), 8148, doi:10.1029/2001JD000438.

Zebker, H., S. Hensley, P. Shanker, and C. Wortham (2010), Geodetically accurate InSAR data processor, *IEEE Trans. Geosci. Remote Sens.*, *48*(12), 4309–4321, doi:10.1109/TGRS.2010.2051333.